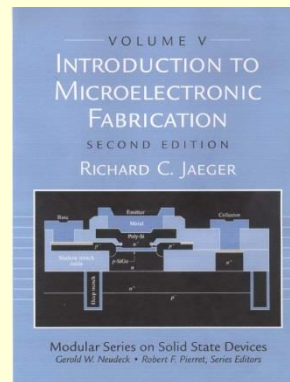


Introduction to Microelectronic Fabrication

Chapter 6 Film Deposition



Evaporation High Vacuum System

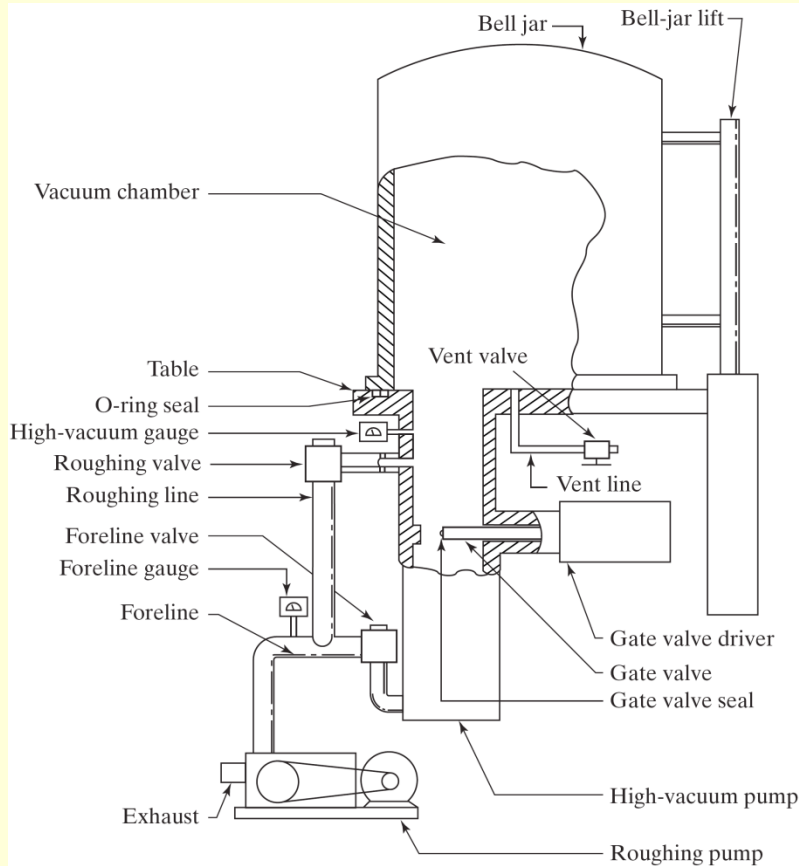
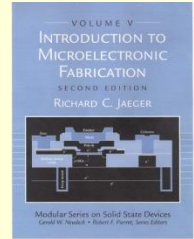
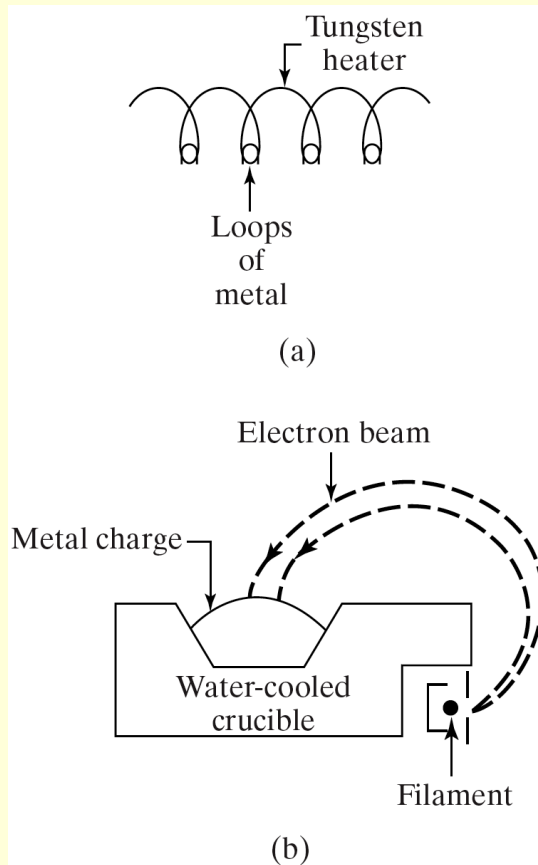
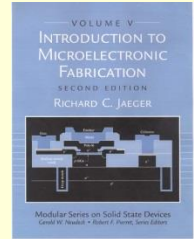


FIGURE 6.1

Typical vacuum system used for evaporation including vacuum chamber, roughing pump, high-vacuum pump, and various valves and vacuum gauges. Copyright 1987 McGraw-Hill Book Company. Reprinted with permission from Ref. [5].

Evaporation Filament & Electron Beam



(a) Filament Evaporation with Loops of Wire Hanging from a Heated Filament (high contamination, not thick film)

(b) High Intensity Electron Beam (15keV) is Focused on Metal Charge by a Magnetic Field

Evaporation Electron Beam

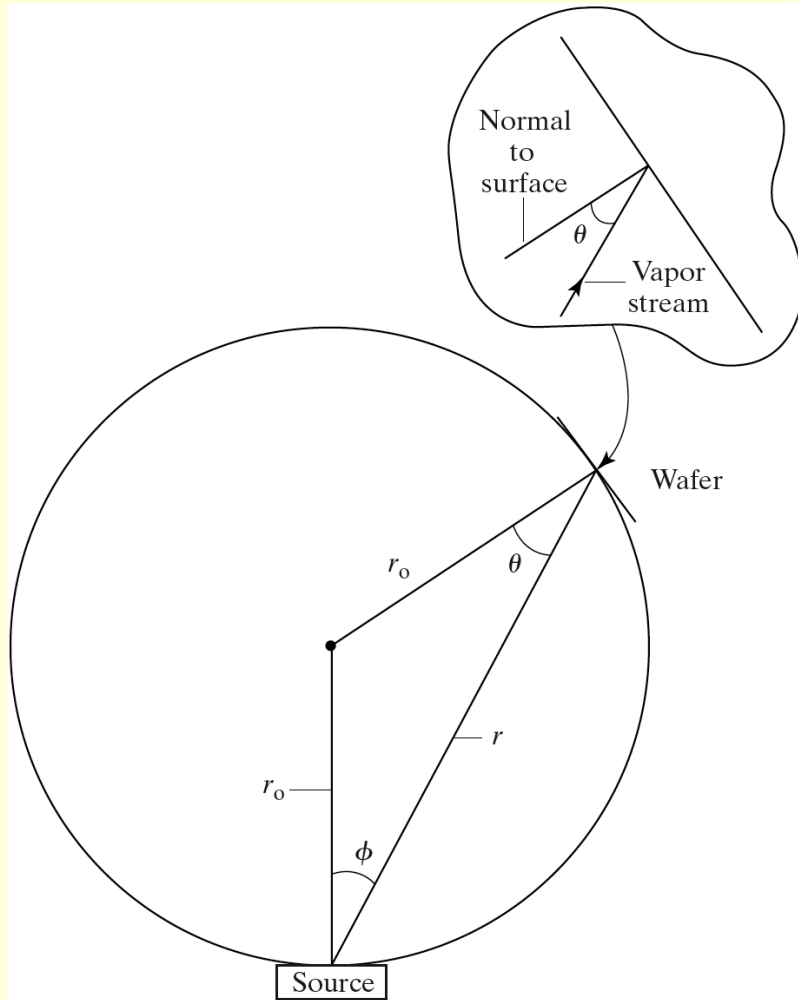
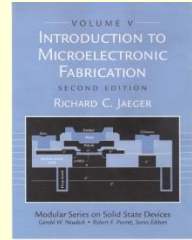


FIGURE 6.4

Photograph of a laboratory E-beam evaporation system with a planetary substrate holder which rotates simultaneously around two axes.

Growth Rate (cm/sec)

$$G = \frac{m}{\pi r^2} \cos \phi \cos \theta$$

$$\cos \phi = \cos \theta = \frac{r}{2r_0}$$

$$G = \frac{m}{4\pi r_0^2}$$

m = mass evaporation rate (g/sec)

ρ = density (g/cm³)

Evaporation

Shadowing and Step Coverage

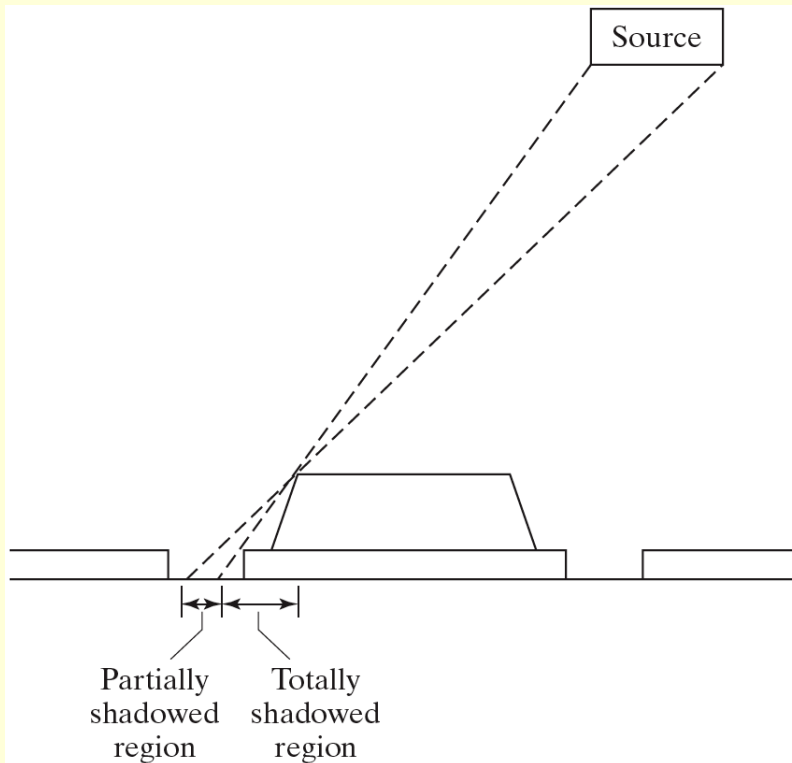
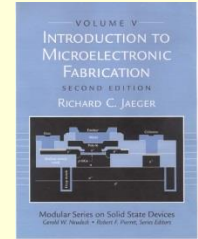


Figure 6.5

- Shadowing and Step Coverage Problems Can Occur in Low Pressure Vacuum Deposition in which the Mean Free Path is Large

Mean Free Path=average distance the molecule travels before it collides with another molecule

$$\lambda = \frac{kT}{\sqrt{2}\pi p d^2}$$

ตัวอย่าง

d=Diameter of gas molecule (2-5Å)

p=Pressure (10^{-4} Pa)

ถ้า d=4Å , p= 10^{-4} Pa, $\lambda \approx 60$ m

Film Deposition

Sputtering

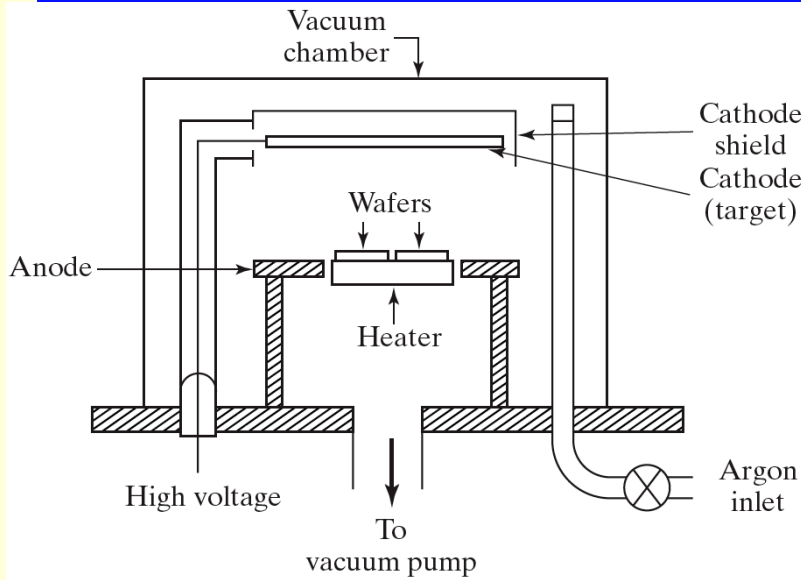
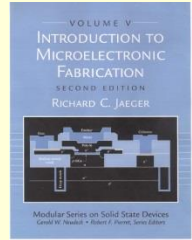


Figure 6.6

A dc sputtering system in which the target material acts as the cathode of a diode and the wafers are mounted on the system anode.

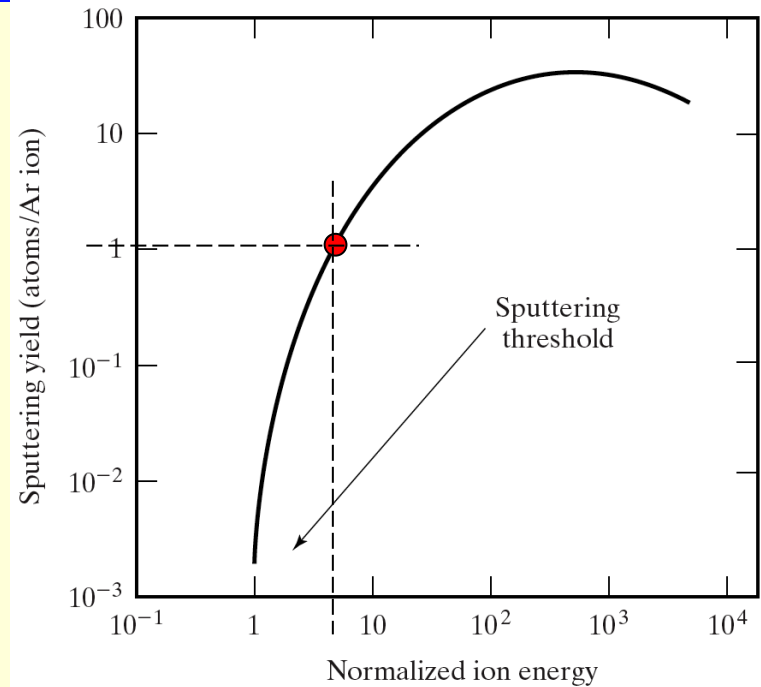


Figure 6.7

Sputtering yield increases rapidly as ion energy is increased above the sputtering threshold (argon)

ตัวอย่าง

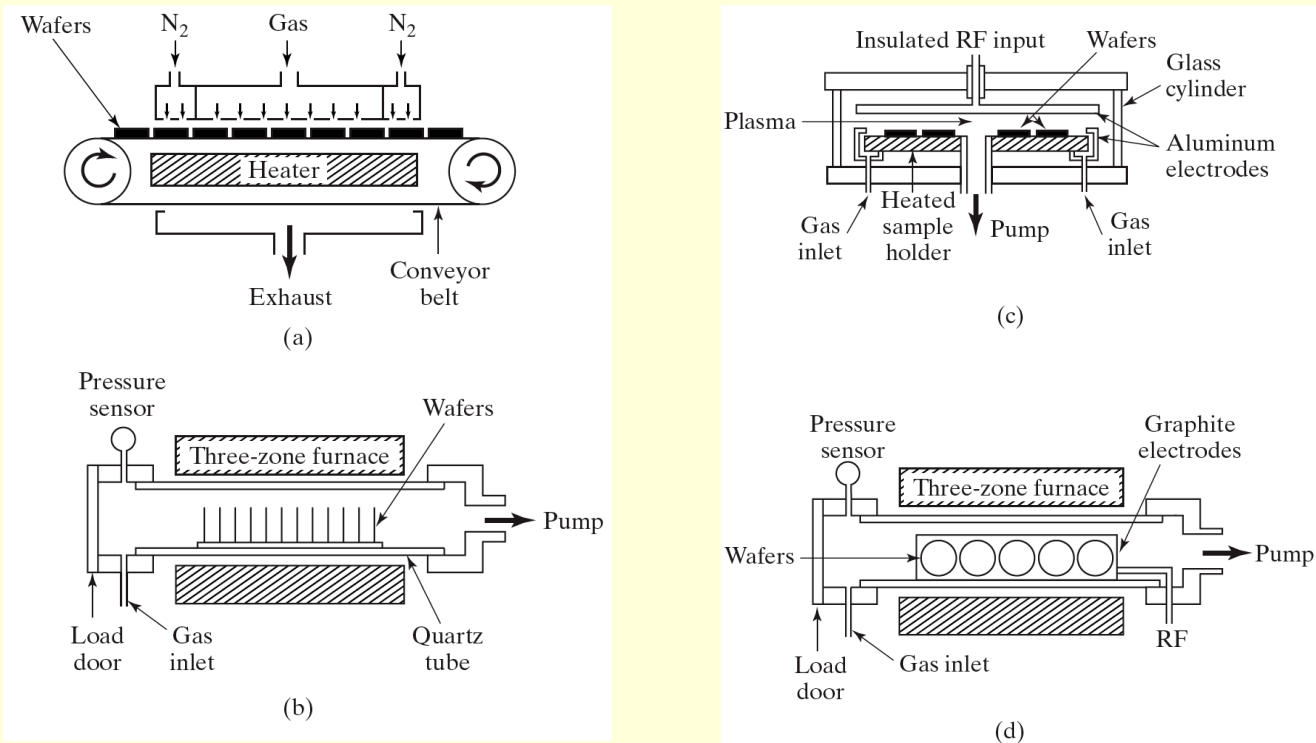
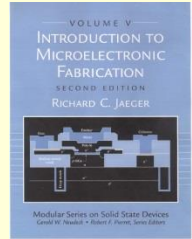
d = Diameter of gas molecule (2-5 Å)

ถ้า $d = 4 \text{ \AA}$, $p = 100 \text{ Pa}$, $\lambda \approx 60 \text{ \mu m}$

$$\lambda = \frac{kT}{\sqrt{2}\pi p d^2}$$

CVD

Chemical Vapor Deposition

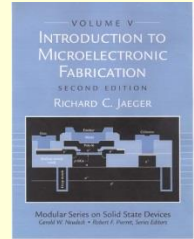


$T=300-1150^{\circ}C$
 30-250 Pa
 SiO_2
 Si_3N_4
 PolySi

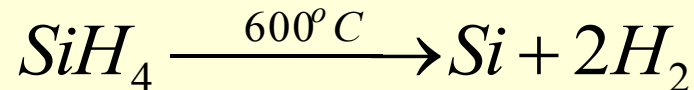
Figure 6.8 Four types of CVD systems. (a) Atmospheric-pressure reactor (b) hot-wall low-pressure (LPCVD) system in a three-zone furnace (c) parallel-plate plasma-enhanced system (d) photo-enhanced (PECVD) system using a three-zone furnace. Copyright 1983 Bell Telephone Laboratories, Inc. Reprinted with permission from Ref. [2].

CVD

Polysilicon Deposition



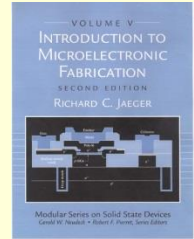
- Low Pressure Chemical Vapor Deposition (LPCVD)
 - 25-150 Pa
- Thermal Decomposition of Silane
 - 100% Silane
 - 20-30% Silane in Nitrogen



- 100-200 Å/min at 600-650° C

CVD

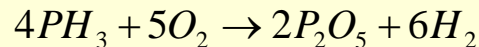
Silicon Dioxide Deposition



Deposition of Silicon Dioxide over Aluminum (300 - 500 C)



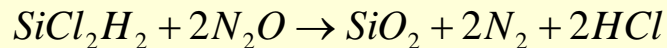
Phosphorus Doped SiO_2 - Atmospheric Pressure or LPCVD



SiO_2 containing 6-8% phosphorus will soften and flow at 1000-1100° C.

Higher Temperature Prior to Metallization

Dichlorosilane Reaction at 900° C



“P-glass reflow” can be used to smooth surface topology.

LPCVD Decomposition of TEOS 650 - 750° C



Film Deposition

Deposited Oxide Properties

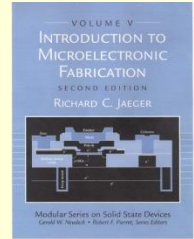
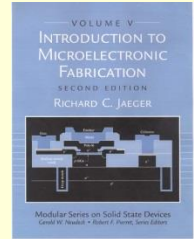


TABLE 6.1 Properties of Various Deposited Oxides (After ref. [2])

Source	Deposition Temperature (°C)	Composition	Conformal Step Coverage	Dielectric Strength (MV/cm)	Etch Rate (Å/min) [100:1 H ₂ O:HF]
Silane	450	SiO ₂ (H)	No	8	60
Dichlorosilane	900	SiO ₂ (Cl)	Yes	10	30
TEOS	700	SiO ₂	Yes	10	30
Plasma	200	SiO _{1.9} (H)	No	5	400

CVD

Silicon Nitride

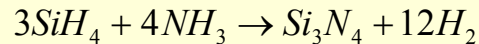


Silicon Nitride

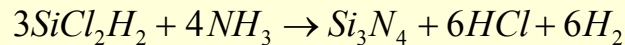
Oxidation Mask for Recessed Oxidation

Final Passivation Layer Over Die Surface

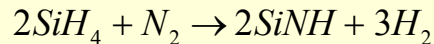
Silane Reaction with Ammonia - 700 - 900°C at Atmospheric Pressure



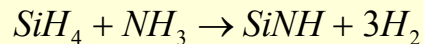
Dichlorosilane Reaction - LPCVD at 700 - 800°C



Plasma Reaction of Silane with Nitrogen

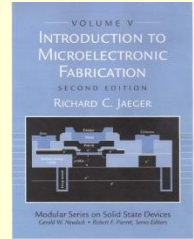


Plasma Reaction of Silane with Ammonia (Argon Plasma)

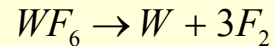


CVD

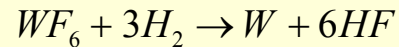
Metal Deposition (Mo, Ta, Ti, W)



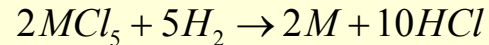
Tungsten - Thermal, Plasma or Optical Assisted Decomposition of WF_6



Tungsten - Reduction of WF_6 with Hydrogen



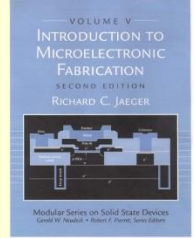
Mo, Ta and Ti - LPCVD Reaction with Hydrogen



Copper is Deposited by "Standard" Plating Techniques

Film Deposition

Epitaxial Growth



- Vapor Phase Epitaxy
- Liquid Phase Epitaxy
 - Compound Semiconductors
- Molecular Beam Epitaxy
 - Compound Semiconductors
- III-V Compound Semiconductors
 - GaAs, InP, GaInAs, InAs ...

End of Chapter 6

Epitaxial Growth

Vapor Phase Epitaxy

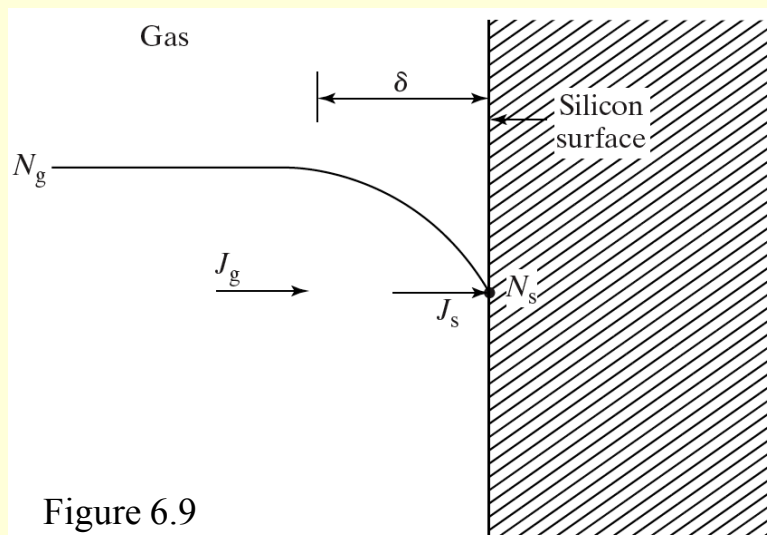
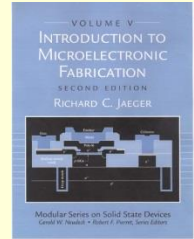


Figure 6.9

Gas diffuses from gas stream and reacts at the surface

$$J_s = k_s N_s \quad J_g = \left(\frac{\overline{D}_g}{\delta} \right) (N_g - N_s) = h_g (N_g - N_s)$$

$$J_s = J_g$$

$$\text{Growth Rate} \quad v = \frac{J_s}{N} = \frac{k_s h_g}{k_s + h_g} \frac{N_g}{N}$$

$$\text{Mass Transfer Limited: } v \cong h_g \frac{N_g}{N} \quad \text{for } k_s \gg h_g$$

$$\text{Surface Reaction Limited : } v \cong k_s \frac{N_g}{N} \quad \text{for } h_g \gg k_s$$

Epitaxial Growth Growth Rates

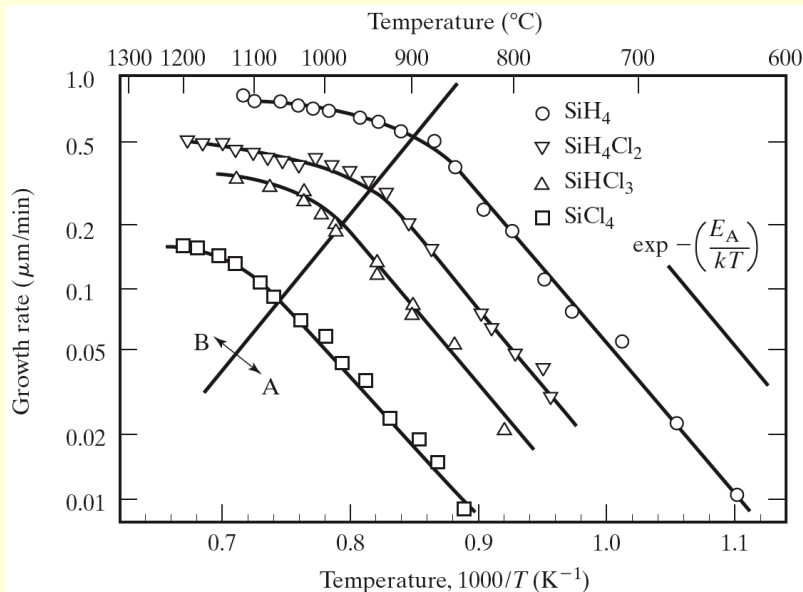
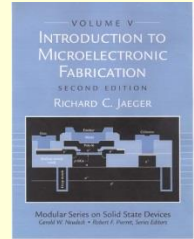
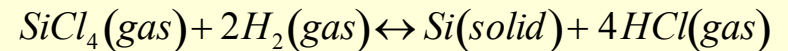


Figure 6.10

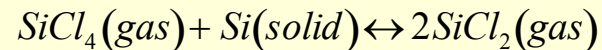
Temperature dependence of the silicon epitaxial growth process for four different sources. The growth is surface-reaction-limited in region A and is mass-transfer-limited in region B. Reprinted with permission from Philips Journal of Research from Ref. [3].

Reversible Deposition Process at 1200° C

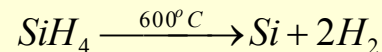


HCl in Input Stream can be Used to Clean Surface

Competing Etching Reaction



Alternative - Pyrolytic Decomposition of Silane



Epitaxial Growth Vapor Phase Systems

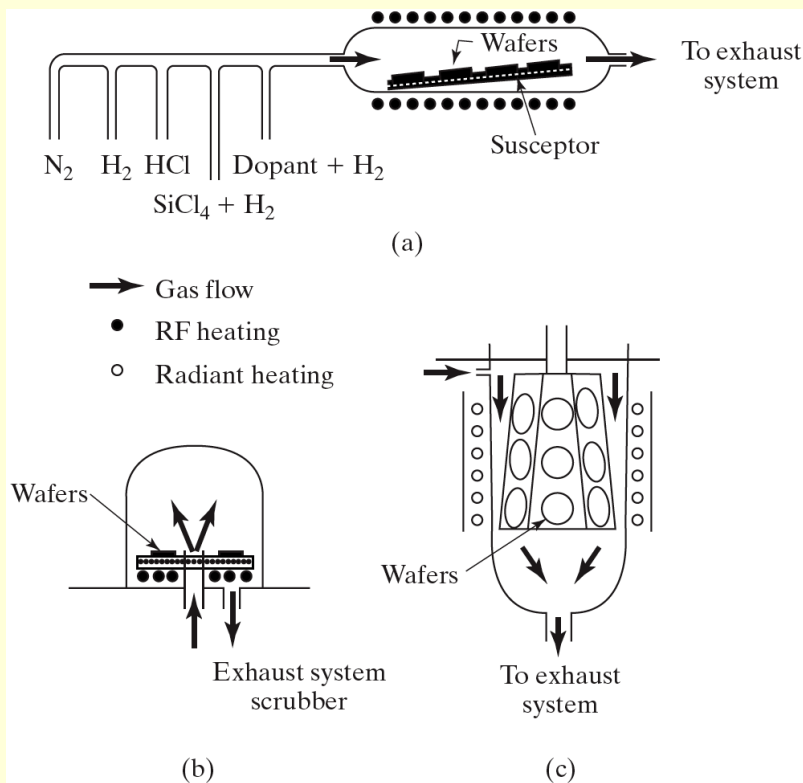
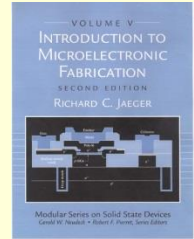
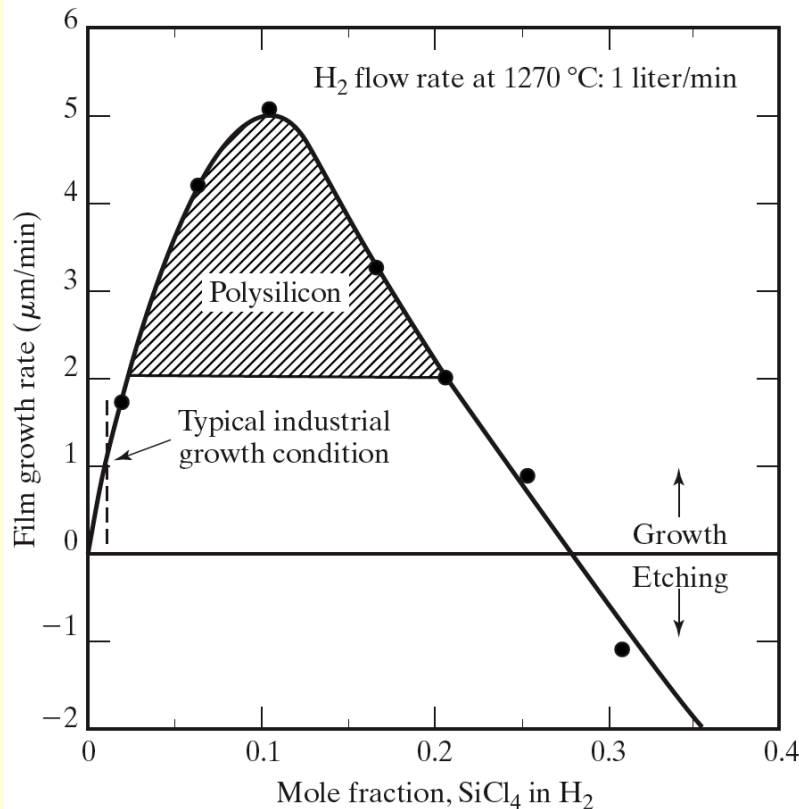
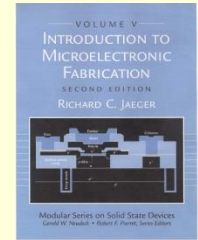


FIGURE 6.11

(a) Horizontal, (b) pancake, and (c) barrel susceptors commonly used for vapor-phase epitaxy. Copyright 1985 John Wiley & Sons, Inc., with permission from Ref. [1].

Epitaxial Growth

Growth in Silicon Tetrachloride



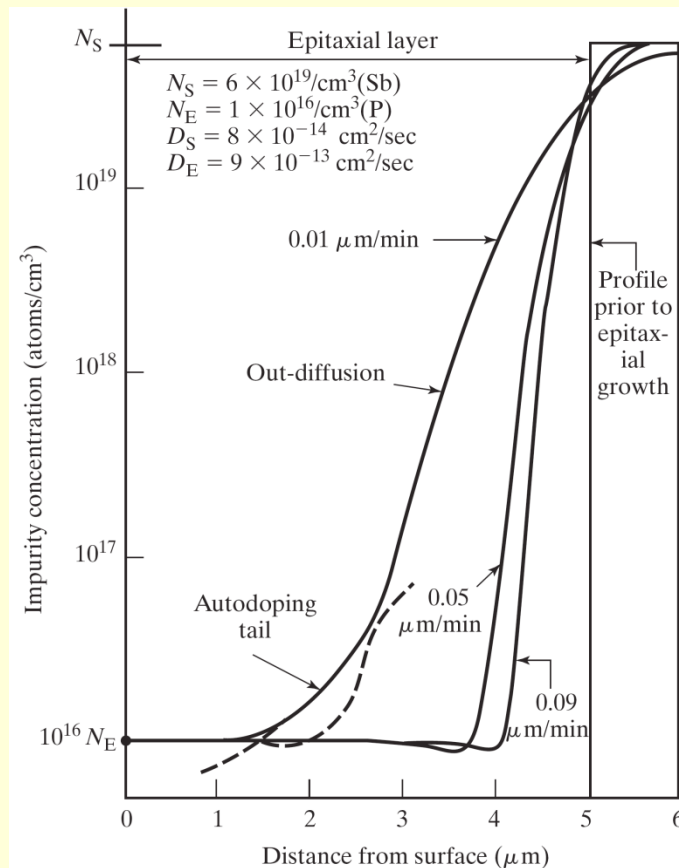
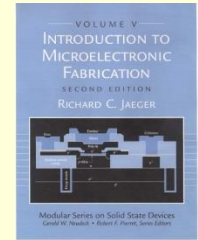
Single Crystal Silicon Growth for Rates Below 2 $\mu\text{m}/\text{min}$

Etching for High SiCl_4 Concentrations

FIGURE 6.12

Silicon epitaxial growth rate as a function of SiCl_4 concentration. Polysilicon deposition occurs for growth rates exceeding 2 $\mu\text{m}/\text{min}$. Etching of the surface will occur for mole fraction concentrations exceeding 28%. Copyright 1985 John Wiley & Sons, Inc, with permission from Ref. [1].

Epitaxial Growth Impurity Redistribution



Moving Boundary Diffusion Problem

$$D \frac{\partial^2 N}{\partial x^2} = \frac{\partial N}{\partial t} + v_x \frac{\partial N}{\partial x}$$

FIGURE 6.13

Redistribution of impurity atoms due to gas-phase autodoping and impurity out-diffusion during epitaxial layer growth. Out-diffusion is calculated using eq. (6.33) for epitaxial growth of a phosphorus-doped layer at 1150 °C over an antimony-doped buried layer with a surface concentration of $6 \times 10^{19}/\text{cm}^3$. The three curves are for growth rates of 0.01, 0.05, and 0.09 $\mu\text{m}/\text{min}$. For clarity, the effects of autodoping are shown on only one curve.

Epitaxial Growth Geometrical Model

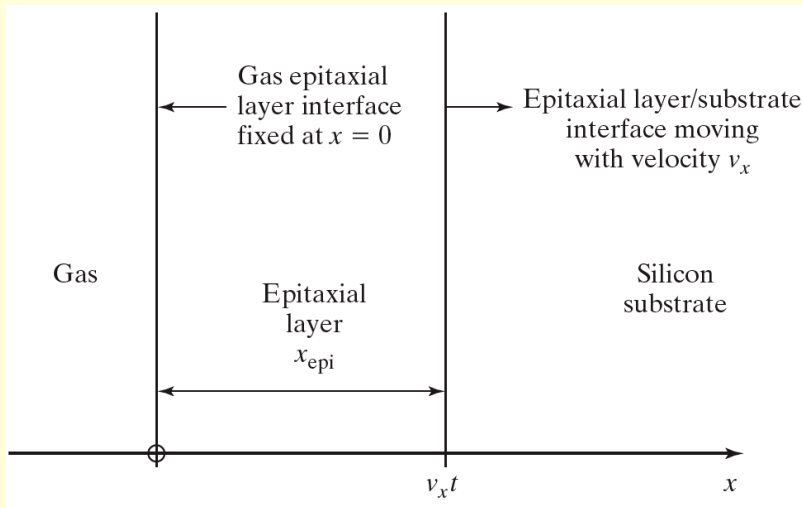
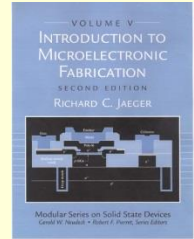


Figure 6.4

$$D \frac{\partial^2 N}{\partial x^2} = \frac{\partial N}{\partial t} + v_x \frac{\partial N}{\partial x}$$

Solution is Superposition of Two Cases

$$N(x, t) = N_1(x, t) + N_2(x, t)$$

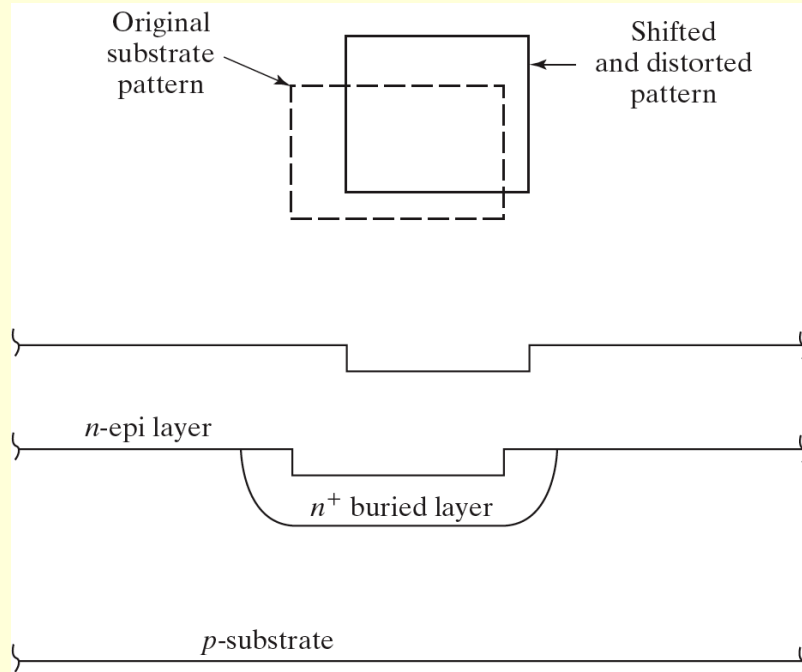
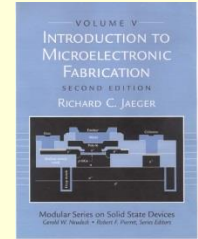
Undoped Epi-Layer on Uniformly Doped Substrate

$$N_1(x, t) = \frac{N_S}{2} \left[1 + \operatorname{erf} \left(\frac{x - x_{epi}}{2\sqrt{D_S t}} \right) \right]$$

Doped Epi-Layer on Undoped Substrate

$$N_2(x, t) = \frac{N_E}{2} \left[1 + \operatorname{erfc} \left(\frac{x - x_{epi}}{2\sqrt{D_E t}} \right) \right] + \exp \frac{v_x x}{D_E} \operatorname{erfc} \left(\frac{x + x_{epi}}{2\sqrt{D_E t}} \right)$$

Epitaxial Growth Pattern Shift

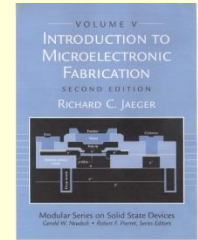


- Pattern Shift During Epitaxial Growth Over an n^+ Buried Layer.
- Pattern is Both Shifted and Distorted in Shape

Figure 6.15

Film Deposition

References & Further Reading



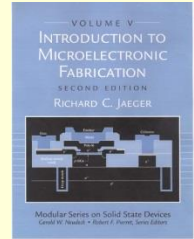
REFERENCES

- [1] S. M. Sze, *Semiconductor Devices—Physics and Technology*, John Wiley & Sons, New York, 1985.
- [2] A. C. Adams, "Dielectric and Polysilicon Film Deposition," Chapter 3 in S. M. Sze, Ed., *VLSI Technology*, McGraw-Hill, New York, 1983.
- [3] F. C. Eversteyn, "Chemical-Reaction Engineering in Semiconductor Industry," *Philips Research Reports*, 29, 45–66 (February, 1974).
- [4] A. B. Glaser and G. E. Subak-Sharpe, *Integrated Circuit Engineering*, p. 205–209, Addison-Wesley, Reading, MA, 1979.
- [5] W. S. Ruska, *Microelectronic Processing*, McGraw-Hill, New York, 1987.

FURTHER READING

- [1] J. L. Vossen and W. Kern, Eds., *Thin Film Processes*, Academic Press, New York, 1978.
- [2] J. F. O'Hanlon, *A User's Guide to Vacuum Technology*, John Wiley & Sons, New York, 1980.
- [3] L. Holland, *Vacuum Deposition of Thin Films*, John Wiley & Sons, New York, 1961.
- [4] A. S. Grove, *Physics and Technology of Semiconductor Devices*, John Wiley & Sons, New York, 1967.
- [5] H. C. Theuerer, "Epitaxial Silicon Films by Hydrogen Reduction of SiCl_4 ," *Journal of the Electrochemical Society*, 108, 649–653 (July, 1961).
- [6] C. O. Thomas, D. Kahng, and R. C. Manz, "Impurity Distribution in Epitaxial Silicon Films," *Journal of the Electrochemical Society*, 109, 1055–1061 (November, 1962).
- [7] A. S. Grove, A. Roder, and C. T. Sah, "Impurity Distribution in Epitaxial Growth," *Journal of Applied Physics*, 36, 802–810 (March, 1965).
- [8] D. Kahng, C. O. Thomas, and R. C. Manz, "Epitaxial Silicon Junctions," *Journal of the Electrochemical Society*, 110, 394–400 (May, 1963).
- [9] W. H. Shepherd, "Vapor Phase Deposition and Etching of Silicon," *Journal of the Electrochemical Society*, 112, 988–994 (October, 1965).
- [10] G. R. Srinivasan, "Autodoping Effects in Silicon Epitaxy," *Journal of the Electrochemical Society*, 127, 1334–1342 (June, 1980).
- [11] J. C. Bean, "Silicon Molecular Beam Epitaxy as a VLSI Processing Technique," 1981 *IEEE IEDM Proceedings*, p. 6–13.

Copyright Notice



- © 2002 Pearson Education, Inc., Upper Saddle River, NJ. All rights reserved. This material is protected under all copyright laws as they currently exist. No portion of this material may be reproduced, in any form or by any means, without permission in writing from the publisher.
- For the exclusive use of adopters of the book Introduction to Microelectronic Fabrication, Second Edition by Richard C. Jaeger. ISBN0-201-44494-1.

End of Chapter 6